Kinematical Bound States of Steps Caused by Asymmetry in Step Kinetics

著者	Sato Masahide, Uwaha Makio
journal or publication title	Journal of the Physical Society of Japan
volume	66
number	4
page range	1054-1062
year	1997-07-01
URL	http://hdl.handle.net/2297/25294

doi: 10.1143/JPSJ.66.1054

Journal of the Physical Society of Japan
Vol. 66, No. 4, April, 1997, pp. 1054-1062

Kinematical Bound States of Steps Caused by Asymmetry in Step Kinetics

Masahide SATO and Makio UWAHA

Department of Physics, Nagoya University, Furo-cho, Chikusa-ku, Nagoya 464-01

(Received September 19, 1996)

We study time evolution of parallel straight steps with repulsive interaction between steps. If step kinetics is asymmetric in the upper and the lower terraces (Schwoebel effect), a vicinal face becomes unstable when undersaturation exceeds a critical value, and an array of large bunches described by the Benney equation appears. In the one-sided model (the extreme limit of the asymmetry) a pairing instability occurs. In this case the instability always ends up with formation of step pairs, and with large undersaturation hierarchical bound states of step pairs are formed. On the contrary many-body bound states appear in the general asymmetric model.

KEYWORDS: step bunching, Schwoebel effect, Benney equation, surface diffusion

§1. Introduction

Asymmetry of the surface diffusion field in the front and in the back of a step can cause a bunching instability. In the case of Si(111), which is experimentally the best studied system,[1-3] one of the candidates to produce this asymmetry is the drift of adsorbed atoms (adatoms) caused by the electric current which is used for heating the specimen.[4-10] In sublimation the flux of atoms from the step onto the upper terrace is different from that onto the lower terrace because of the drift. This asymmetry makes an equidistant step train unstable, and a bunching occurs. If the distance between steps is larger than the surface diffusion length, the drift in the step-up direction makes the step train unstable. In the opposite case the drift in the step-down direction makes the step train unstable. Near the critical point the instability occurs at long wavelengths. We can take the continuum limit and derive a nonlinear evolution equation for the step density.[9,10] The result is a form of the Benney equation.[11-14] The Benny equation interpolates the Kuramoto-Sivashinsky (KS) equation,[15-17] which exhibits spatiotemporal chaos, and the Korteweg-de Vries (KdV) equation. The solution of the Benney equation with a large dispersion term produces an array of soliton-like pulses, which corresponds to the appearance of a train of large step bunches.

The drift of adatoms is a characteristic effect for Si, whereas bunching is a general phenomenon. Asymmetry in the step kinetics (Schwoebel effect[18,19]), which exists in many systems, also produces an asymmetry in the surface diffusion field. When atoms are detached from a step only to the lower terrace (i.e. the one-sided model), a paring instability occurs in sublimation with undersaturation exceeding a critical strength,[20] and a equidistant step train becomes unstable to pair formation.[21] The critical undersaturation for the instability is determined by competition between the surface diffusion and the repulsive interaction of steps. The one-sided model is the extreme limit of the asymmetric step kinetics, and the above features of the instability are expected to change with general asymmetry.[22,23] When atoms can detach from the step onto both terraces with different kinetic coefficients, the fluctuation of step distances at a long wavelength first becomes unstable instead of pairing. In such circumstances we can derive a similar continuum equation for the step density as in the bunching by drift of adatoms.

In this paper we study the change of step behavior with the change of asymmetry in step kinetics. We use the standard step flow model of Burton, Cabrera and Frank[24] with the asymmetric step kinetics and the step interaction taken into account. The model is described in §2. When the Schwoebel effect is sufficiently strong and the step kinetics for both side terraces is fast, the instability of a vicinal face occurs at long wavelengths, which is summarized in §3. In the one-sided model, that is the limit of strong Schwoebel effect, the appearance of instability changes: a pairing instability occurs at first. In §4 we study the instability numerically, and show an appearance of hierarchical bound states of step pairs. In §5 we investigate the effect of general asymmetry, which causes many-body bound states. A condition for the formation of a three-body bound state is derived and the velocity of the bound steps is found.

§2. Model

We use the standard vapor growth model of Burton, Cabrera and Frank[24] to obtain the velocity of a step. Atoms impinge from an ambient gas phase to the crystal surface at the frequency f per unit area. Atoms on the surface (we call adatoms) diffuse with the diffusion coefficient D_s and evaporate to the ambient phase at the rate $1/\tau$. The adatom density obeys the diffusion equation

$$\frac{\partial c}{\partial t} = D_s \nabla^2 c - \frac{1}{\tau} c + f. \tag{2.1}$$

We assume that all steps are parallel and straight. The

linear analysis[25,26] shows that steps have a tendency to be straight in the bunching instability. Also the study of a simplified two-dimensional model[27] suggests that the essential physics of bunching can be extracted in a one-dimensional model. We take the y-axis in the step-down direction, and the position of the nth step as $y = y_n$. In sublimation the steps recede by desorbing atoms onto the upper and the lower terraces, while they advance by absorbing adatoms in growth. The flux of adatoms from both terraces to the step is proportional to the difference of adatom density at the step and that of local equilibrium c_n:

$$\pm D_s \left.\frac{\partial c}{\partial y}\right|_{y_n \pm 0} = K_\pm [c(y_n \pm 0) - c_n], \tag{2.2}$$

where $K_+(K_-)$ represents the kinetic coefficient of the lower (upper) side terrace.[28] The local equilibrium adatom density at the nth step is different from that at an isolated step c_{eq}^0 by an amount proportional to the spatial derivative of the step interaction energy ζ_n. When the adatom density is low ($\Omega c_{eq}^0 \ll 1$), c_n is expressed as[20,29]

$$c_n = c_{eq}^0 + \frac{c_{eq}^0 \Omega}{k_B T} \frac{\partial \zeta_n}{\partial y_n}, \tag{2.3}$$

where Ω is the atomic area, k_B is the Boltzmann constant and T is temperature. If steps are interacting with a power-law potential, the interaction energy of the nth step can be written as

$$\zeta_n = A \sum_{m \neq n} |y_n - y_m|^{-\nu}, \tag{2.4}$$

where the strength of step interaction A is positive for repulsion. In the case of elastic repulsion[30] $\nu = 2$, which is used for the numerical study in this paper.

We solve the diffusion equation (2.1) with the boundary conditions (2.2) in the static approximation: $\partial c/\partial t = 0$. By using the width of both lower and upper terraces $l_{n\pm} = |y_n - y_{n\pm1}|$, the velocity of the nth step is given by[20-22]

$$\begin{aligned} v_n &= \Omega D_s \left.\frac{dc}{dy}\right|_{y_n+0} - \Omega D_s \left.\frac{dc}{dy}\right|_{y_n-0} \\ &= \Omega \frac{D_s}{x_s} \frac{[\cosh(l_{n+}/x_s) + \lambda_- \sinh(l_{n+}/x_s)](c_\infty - c_n) - (c_\infty - c_{n+1})}{(\lambda_+ + \lambda_-)\cosh(l_{n+}/x_s) + (1 + \lambda_+\lambda_-)\sinh(l_{n+}/x_s)} \\ &\quad + \Omega \frac{D_s}{x_s} \frac{[\cosh(l_{n-}/x_s) + \lambda_+ \sinh(l_{n-}/x_s)](c_\infty - c_n) - (c_\infty - c_{n-1})}{(\lambda_+ + \lambda_-)\cosh(l_{n-}/x_s) + (1 + \lambda_+\lambda_-)\sinh(l_{n-}/x_s)}, \end{aligned} \tag{2.5}$$

where x_s ($\equiv \sqrt{D_s \tau}$) is the surface diffusion length, c_∞ ($\equiv f\tau$) the adatom density far from the step, and $\lambda_\pm$($\equiv D_s/x_s K_\pm$) the dimensionless resistances of step kinetics. The static approximation is valid when the step velocity v_n is small as $|D_s \nabla^2 c| \gg |v_n \nabla c|$, which is satisfied when $\Omega|c_\infty - c_{eq}| \ll 1$ (or $\Omega|c_\infty - c_{eq}|l/x_s \ll 1$ when $l \ll x_s$). With a Green's function approach it is shown[31] that the result of a time dependent analysis does not give any qualitative difference from that of the static approximation.

In general the step kinetics with both terraces are not the same. The asymmetry of the kinetics, which means $K_+ \neq K_-$, is called the Schwoebel effect[18,19] or diffusion barrier,[32] and plays an important roll in morphological instability of steps.[22,28] Since in many cases adatoms on the lower terrace are incorporated into the step more easily than those on the upper terrace, we assume for definiteness $\lambda_- > \lambda_+$ ($K_- < K_+$) from now on. With this asymmetry the instability occurs in sublimation when the undersaturation exceeds a critical value. If the asymmetry of the step kinetics is the opposite sense, the instability occurs in growth.

In the following analysis we use dimensionless variables. By using x_s as the length scale and t_s($\equiv \tau x_s^3 k_B T/2A\Omega^2 c_{eq}^0$: we also assume $\nu = 2$) as the time scale, that is $\tilde{y} = y/x_s$ and $\tilde{t} = t/x_s$, the dimensionless velocity $\tilde{v}_n$ is expressed as

$$\begin{aligned} \tilde{v}_n = &\frac{(\cosh \tilde{l}_{n+} + \lambda_- \sinh \tilde{l}_{n+})\tilde{f}_n - \tilde{f}_{n+1}}{(\lambda_+ + \lambda_-)\cosh \tilde{l}_{n+} + (1 + \lambda_+\lambda_-)\sinh \tilde{l}_{n+}} \\ &+ \frac{(\cosh \tilde{l}_{n-} + \lambda_+ \sinh \tilde{l}_{n-})\tilde{f}_n - \tilde{f}_{n-1}}{(\lambda_+ + \lambda_-)\cosh \tilde{l}_{n-} + (1 + \lambda_+\lambda_-)\sinh \tilde{l}_{n-}}, \end{aligned} \tag{2.6}$$

where $\tilde{l}_{n\pm}$ ($\equiv |\tilde{y}_n - \tilde{y}_{n\pm1}|$) are the dimensionless terrace widths and $\tilde{f}_n$ ($\equiv \Omega(c_\infty - c_n)\tau/t_s$) is the dimensionless supersaturation, which is given by

$$\tilde{f}_n = \tilde{f} + \sum_{m \neq n} (\tilde{y}_n - \tilde{y}_m)^{-3}. \tag{2.7}$$

$\tilde{f}$ ($\equiv \Omega(c_\infty - c_{eq}^0)t_s/\tau$) represents the strength of supersaturation (when $\tilde{f} > 0$) or undersaturation ($\tilde{f} < 0$). The second term of eq. (2.7) is the effect of the repulsive interaction, which produces the difference of the supersaturation (undersaturation) of each step from that of an isolated step.

§3. Instability of a Vicinal Face

In this section we summarize the study of instability of a vicinal face with a small step distance $\tilde{l} \ll 1$ ($l \ll x_s$).[21-23] Consider an infinite array of equidistant steps and shift the nth step from the unperturbed position by $\delta\tilde{y}_n = \delta\tilde{y}_{\tilde{k}} e^{(\tilde{\omega}_{\tilde{k}}\tilde{t} + in\tilde{k}\tilde{l})}$, where $\tilde{k}(\equiv kx_s)$ is the dimensionless wave number. The growth rate of the perturbation $\tilde{\omega}_{\tilde{k}}$ can be calculated from eq. (2.5). For simplicity we assume in this section a step interacts only with its nearest neighbors. When we take account of the lowest order terms in $\tilde{l}$ with respect to the surface diffusion length, $\tilde{\omega}_{\tilde{k}}$ is given by

$$\tilde{\omega}_{\tilde{k}} = \frac{\lambda_+ - \lambda_-}{\lambda_+ + \lambda_-}(1-\cos\tilde{k}\tilde{l})\tilde{f} - \frac{4\phi''(\tilde{l})}{\lambda_+ + \lambda_-}(1-\cos\tilde{k}\tilde{l})^2 - 2\tilde{l}\phi''(\tilde{l})(1-\cos\tilde{k}\tilde{l})\left[1-2\frac{1+\lambda_+\lambda_-}{(\lambda_+ + \lambda_-)^2}(1-\cos\tilde{k}\tilde{l})\right] + \mathrm{i}\tilde{f}\sin\tilde{k}\tilde{l}, \tag{3.1}$$

where $\phi(\tilde{l})$ is the scaled potential, which is given by $\phi(\tilde{l}) = \tilde{l}^{-2}/2$ for the elastic repulsion. Since we assume that $\lambda_- > \lambda_+$, the equidistant step train becomes unstable when the undersaturation exceeds the critical value

$$\tilde{f}_c = -2\frac{\lambda_- + \lambda_+}{\lambda_- - \lambda_+}\tilde{l}\phi''(\tilde{l}), \tag{3.2}$$

which is obtained from the coefficient of $\tilde{k}^2$ term by expanding eq. (3.1). Since the coefficient of $\tilde{k}^4$ term is positive, the instability starts at $\tilde{k} \approx 0$.

Near the critical point the wavelength of the unstable modes are much longer than the step distance. We can take the continuum limit of the discrete step model and derive an evolution equation for the step density $\tilde{\rho}$ ($\equiv \tilde{l}^{-1}$) from the continuity equation $\partial\tilde{\rho}/\partial\tilde{t} + \partial(\tilde{\rho}\tilde{v})/\partial\tilde{y} = 0$.[23] For the sinusoidal perturbation $\delta\tilde{\rho} = \delta\tilde{\rho}_{\tilde{k}}\mathrm{e}^{(\mathrm{i}\tilde{k}\tilde{y}+\tilde{\omega}_{\tilde{k}}\tilde{t})}$ to the step density, the linear dispersion relation is obtained as

$$\tilde{\omega}_{\tilde{k}} = -\frac{\lambda_+\lambda_-}{\lambda_+ + \lambda_-}\frac{\tilde{f}}{\tilde{\rho}_0^2}\mathrm{i}\tilde{k} - \frac{1}{3!}\frac{\tilde{f}}{\tilde{\rho}_0^3}\mathrm{i}\tilde{k}^3 - \left(\frac{\mathrm{d}\tilde{\zeta}}{\mathrm{d}\tilde{\rho}_0} + \frac{1}{2!}\frac{\lambda_- - \lambda_+}{\lambda_- + \lambda_+}\frac{\tilde{f}}{\tilde{\rho}_0{}^2}\right)\tilde{k}^2 - \frac{1}{\lambda_- + \lambda_+}\frac{1}{\tilde{\rho}_0}\frac{\mathrm{d}\tilde{\zeta}}{\mathrm{d}\tilde{\rho}_0}\tilde{k}^4, \tag{3.3}$$

where $\tilde{\zeta}(\tilde{\rho})$ is the scaled interaction energy, which is related to the pair potential as $\partial\tilde{\zeta}/\partial\tilde{\rho} = \tilde{l}^3(\partial^2\phi/\partial\tilde{l}^2)$.[34,35] Note that the average dimensionless step density is large: $\tilde{\rho}_0 \gg 1$. The first term of eq. (3.3) does not appear if one expands eq. (3.1)[22] because it comes from the higher order expansion of eq. (2.6) in $\tilde{l}(= l/x_s)$. The instability occurs if

$$\tilde{f} < \tilde{f}_c \equiv -2\frac{\lambda_- + \lambda_+}{\lambda_- - \lambda_+}\tilde{\rho}_0^2\frac{\mathrm{d}\tilde{\zeta}}{\mathrm{d}\tilde{\rho}_0}. \tag{3.4}$$

The results, eq. (3.3) and eq. (3.4) agree with those of the discrete model, eqs. (3.1) and (3.2).

To study nonlinear effects near the critical point, we introduce the small expansion parameter ϵ ($\equiv 1 - \tilde{f}_c/\tilde{f}$), which represents the distance from the critical point of instability. As is easily seen from eq. (3.3), the wave number of the most unstable mode is proportional to $\sqrt{\epsilon}$ and its growth rate is proportional to ϵ^2. In order to eliminate the explicit ϵ-dependence we introduce new variables,[36]

$$Y \equiv \sqrt{(\lambda_+ + \lambda_-)\tilde{\rho}_0\epsilon}\left(\tilde{y} - \frac{\lambda_+\lambda_-}{\lambda_+ + \lambda_-}\frac{\tilde{f}}{\tilde{\rho}_0^2}\tilde{t}\right), \tag{3.5}$$

$$T \equiv (\lambda_+ + \lambda_-)\tilde{\rho}_0\epsilon^2\frac{\mathrm{d}\tilde{\zeta}}{\mathrm{d}\tilde{\rho}_0}\tilde{t}. \tag{3.6}$$

When the growing fluctuation of the step density becomes $\delta\tilde{\rho} \sim O(\epsilon^{3/2})$, a nonlinear term of the form $\delta\tilde{\rho}(\partial\delta\tilde{\rho}/\partial Y)$, which emerges from the higher order expansion of eq. (2.6) in $\tilde{l}$, becomes comparable to the linear terms. Adding this term to the linear evolution equation, and by rescaling the fluctuation of step density as

$$N \equiv \frac{4\lambda_+\lambda_-\epsilon^{3/2}}{(\lambda_- - \lambda_+)\sqrt{(\lambda_- + \lambda_+)\tilde{\rho}_0^3}}\delta\tilde{\rho}, \tag{3.7}$$

we obtain the equation for the scaled fluctuation of the step density[23]

$$\frac{\partial N}{\partial T} + \delta\frac{\partial^3 N}{\partial Y^3} + \frac{\partial^4 N}{\partial Y^4} + \frac{\partial^2 N}{\partial Y^2} + N\frac{\partial N}{\partial Y} = 0, \tag{3.8}$$

where δ is given by

$$\delta \equiv \frac{1}{3}\frac{\lambda_- + \lambda_+}{\lambda_- - \lambda_+}\sqrt{\frac{(\lambda_+ + \lambda_-)}{\epsilon\tilde{\rho}_0}}. \tag{3.9}$$

Equation (3.8) is called the Benney equation.[11] The Benney equation interpolates the Kuramoto-Sivashinsky (KS) equation[15-17] ($\delta = 0$), whose solution produces spatiotemporal chaos, and the Korteweg-de Vries (KdV) equation ($\delta \to \infty$ and appropriate rescaling).

The solution of the Benney equation has been investigated numerically with a periodic boundary condition by Kawahara and coworkers.[12-14] When δ is sufficiently large ($\delta > 1.2$), equidistant soliton-like pulses with the same amplitude appear. With small $\delta(< 0.35)$ the interpulse distance fluctuates. When δ becomes even smaller ($\delta < 0.15$), the solution of the Benney equation shows the chaotic behavior as the KS equation. Near the critical point of the instability ϵ is small, and the coefficient of the dispersion term $\partial^3 N/\partial Y^3$ is large. Therefore the step density is expected to show an array of equidistant pulses with the same amplitude, which corresponds to a train of large step bunches as found in the discrete model.

Numerical integration of the Benney equation, in addition to the formation of stable pulses, shows the following features. The steady pattern changes with the change of the initial condition. For large initial fluctuation whose wavelength is equal to the system size the interpulse distance of the steady pattern becomes larger (Fig. 1(b)) than that for the small random initial fluctuation (Fig. 1(a)). Also the direction of the motion of steady pulses changes: the steady pulses move to the left for the random initial fluctuation (Fig. 1(a)), and to the right for the large long wavelength fluctuation (Fig. 1(b)). But in the original frame, $\tilde{y}$ and $\tilde{t}$, the pulses move to the left due to the large first derivative term (the shift in eq. (3.5)). A similar change of periodicity and velocity are obtained in the numerical integration of the discrete model. For the bunches grown from the random initial fluctuation, the velocity is determined by the $\tilde{k}$ term of eq. (3.3) near the critical point, and by the $\tilde{k}^3$ term away from the critical point[22] because of the increase of the wave number of the most unstable mode with increasing undersaturation.

The coefficient of the third derivative δ in eq. (3.8) is positive in the present situation, but can be negative if bunching is due to an external field.[9,10] The change

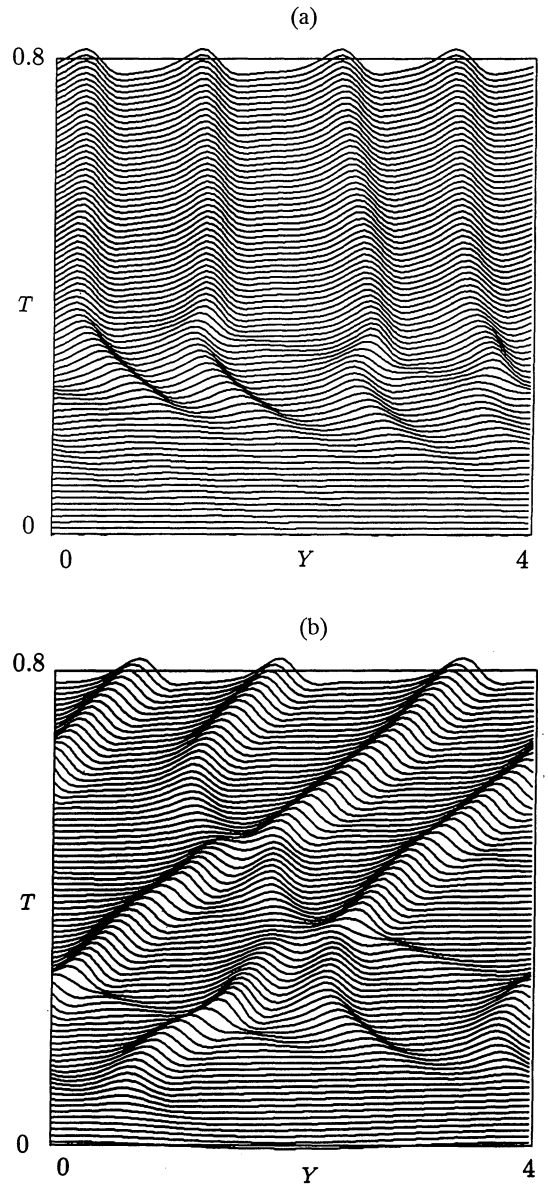

Fig. 1. Evolution of the Benney equation with $\lambda_- = 1$, $\lambda_+ = 10$, $\tilde{\rho}_0 = 8$ and $\epsilon = 0.218$: (a) with random initial fluctuation, (b) with large long wavelength fluctuation.

of sign is equivalent to the replacement N and X by $-N$ and $-X$. Therefore when δ is negative, an array of low step density bands moves to the direction opposite to that with the positive dispersion term in the moving frame.[37]

§4. Bound Sates in the One-Sided Model

Step bunches are formed by continuous "collision" and recombination of steps so that the members of bunch are changing.[22,38] In the following we study the formation of bound states which can sustain themselves without recombination with other steps.

4.1 Pairing of steps

For simplicity and to emphasize the Schwoebel effect, we first assume that only atoms on the lower terrace can solidify at the step and its kinetics is fast: $K_+ \to \infty$, $K_- = 0$ (or $\lambda_- \to \infty$, $\lambda_+ = 0$). In this one-sided model atoms do not move across the step, and the velocity of n-th step is simply given by

$$\frac{\mathrm{d}\tilde{y}_n}{\mathrm{d}\tilde{t}} = \tanh\left(\tilde{y}_{n+1} - \tilde{y}_n\right) \left[\tilde{f} + \sum_{m\neq n} \frac{1}{(\tilde{y}_n - \tilde{y}_m)^3}\right]. \quad (4.1)$$

The first factor is an effective mobility, which is determined by the width of the lower terrace.

If one focuses on the change of a step distance, the effect of diffusion field is equivalent to an effective repulsion in growth and an attraction in sublimation. Suppose that there are two steps, Step 1 and Step 2, with a distance comparable or smaller than the diffusion length ($x_s \geq y_2 - y_1 > 0$). In growth, Step 2 advances faster than Step 1 since it has a larger lower terrace than Step 1, and these steps separate. In sublimation, Step 2 recedes faster than Step 1 and catches up with Step 1. This effective attraction competes with the elastic repulsion, and the steps can form a bound state if c_∞ is so small (i.e. large undersaturation) that $\tilde{f}$ is sufficiently large negative. The critical value of $\tilde{f}$ to form a bound pair is calculated to be $\tilde{f}_c = -8\mathrm{e}^3/27$.[20] At the critical point the distance of the step pair is $\tilde{l}_c = 3/2$, and decreases as $\tilde{f}$ decreases (undersaturation increases). The decrease of the pair size results in the nonlinear velocity of the pair, $\tilde{v}_{\mathrm{pair}} \approx -2|\tilde{f}|^{2/3}$.[20]

This effective attraction through the diffusion field in sublimation also brings about a pairing instability of an equidistant step train (a vicinal face), which is stabilized by the step repulsion under equilibrium or weak undersaturation. The critical value of $\tilde{f}$ for the instability is $\tilde{f}_c = -\pi^4/16\tilde{l}^3$, where $\tilde{l}$ is the initial step distance.[21] This pairing instability is the continuation of the instability of step density given by eq. (3.1). As is easily seen form eq. (3.1), the most unstable mode is $\tilde{k}\tilde{l} = \pi$, that is, a pairing instability occurs first in the one-sided model. With symmetric step kinetics similar pairing instability occurs for noninteracting steps,[39] but the system is stabilized by introducing any long range repulsive interaction.

4.2 Hierarchy of bound states

As shown in §5.2 a bound state consisting of three steps is not stable in the one-sided model, and bachelor steps and bound pairs are basic units. Since the velocity of a bound pair is small, a bachelor step collides with the pair. During the collision the bachelor step combines with one member of the pair and the other old member of the pair is expelled.[20] The bound steps are, in their turn, not independent but interact each other with the diffusion field as well as the elastic strain. If the distance between neighboring pairs is sufficiently smaller than the surface diffusion length x_s, step pairs again can form a bound state. The process of the bound state formation of step pairs (Fig. 2) looks similar to that of the formation of a step pair except that it proceeds much more slowly. If the undersaturation is large enough (or equivalently the repulsion A is small enough or x_s is large enough), even three pairs can form a stable bound state with very large negative $\tilde{f}$.

The bound state consisting of three pairs seems to be the largest in the simulation (yet we have no real proof),

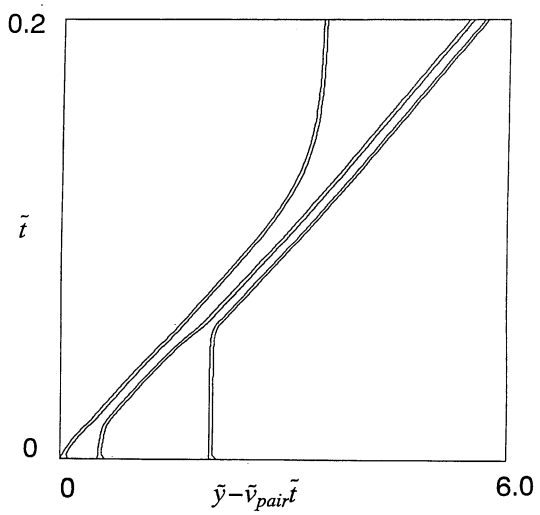

Fig. 2. An example of bound state of pairs with $\tilde{f} = -10^4$ in the reference frame moving with an isolated pair. This process is represented as $\mathbf{2}+\mathbf{1} \to \mathbf{1}+\mathbf{2}$.

and all types of collisions observed are summarized as follows. The collision of a bachelor step with a pair may be expressed as

$$1+1 \to 2, \qquad 2+1 \to 1+2. \tag{4.2}$$

The left hand side of the arrow represents the initial state and the right hand side the final state. With a similar notation (see Fig. 2) the collision of *step pairs* is summarized as follows.

$$\begin{gathered} \mathbf{1}+\mathbf{1} \to \mathbf{2}, \\ \mathbf{2}+\mathbf{1} \to \mathbf{3},\ \mathbf{2}+\mathbf{2} \to \mathbf{1}+\mathbf{3}, \\ \mathbf{3}+\mathbf{1} \to \mathbf{1}+\mathbf{3},\ \mathbf{3}+\mathbf{2} \to \mathbf{2}+\mathbf{3},\ \mathbf{3}+\mathbf{3} \to \mathbf{1}+\mathbf{2}+\mathbf{3}. \end{gathered} \tag{4.3}$$

Each bold number indicates the number of pairs in a bound state, that is $1+1 \to \mathbf{1}$ and $2+2 \to \mathbf{2}$. For example, the last relation in eq. (4.3) implies the following. Two triplet pairs collide since the one on the right is slightly faster. After the collision the one on the left is decomposed into a singlet pair and a doublet pair. These three bound pairs (**1**, **2** and **3**) finally become independent. Collision of a bachelor step with any bound pairs, after recombinations, ends up with an emission of a bachelor step towards the left leaving the bound pairs unchanged:

$$n+1 \to 1+n. \tag{4.4}$$

An example for evolution of a many step system is shown in Fig. 3. Sixty four steps are placed in a cell with a periodic boundary condition with a large undersaturation $\tilde{f} = -8^3 \times 10^4$. The position of steps is plotted in the frame of reference moving with an isolated pair (an orbit of an isolated pair is represented by a pair of vertical lines in the graph), and therefore the actual step position is shifted far to the left in the whole process. Initially, steps are placed with an equal distance with a small random fluctuation. After a very short time, step pairs are formed, and unpaired steps move fast and repeated collisions (recombinations) occur. The paired steps move

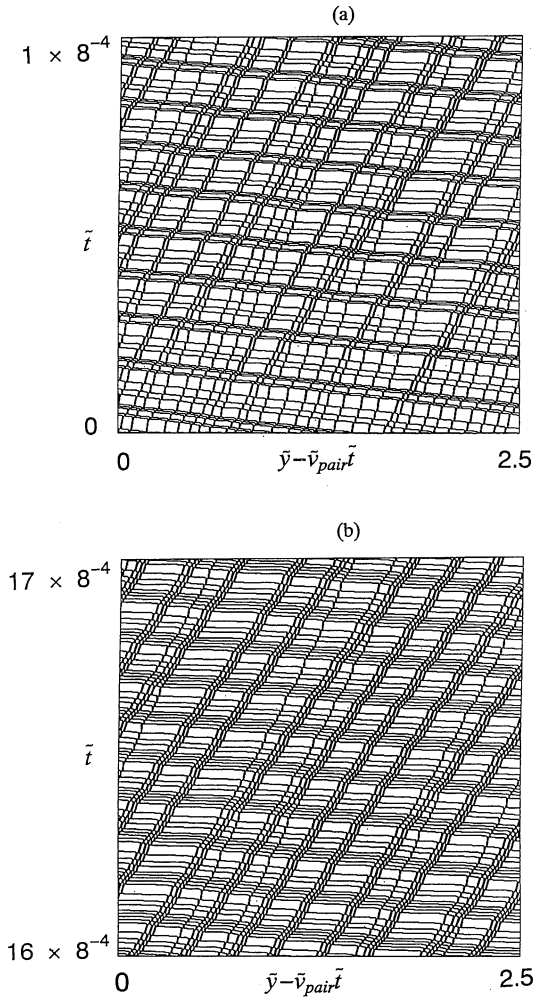

Fig. 3. Evolution of 64 steps in the moving frame. $\tilde{f} = -8^3 \times 10^4$. (a) $0 \le \tilde{t} \le 8^{-4}$ and (b) $16 \times 8^{-4} \le \tilde{t} \le 17 \times 8^{-4}$.

slowly and they start to form three body bound states (Fig. 3(a)). A final steady state combination, which consists of eight triplet pairs, four pairs and eight singles in the present case, is reached after a long time (Fig. 3(b)).

§5. A Few-Body Bound States in the General Asymmetric Model

The one-sided model is the extreme case that emphasizes the asymmetry of step kinetics. In general some features we have seen are expected to change with the strength of the asymmetry. In this section we study the effect of general asymmetry in the step kinetics on bunching instability.

5.1 Pairing instability

First we investigate the occurrence of pairing instability. We assume there are only two steps at $\tilde{y}_1$ and $\tilde{y}_2$ ($\tilde{y}_1 < \tilde{y}_2$) on the crystal surface. By using the distance between two steps $\tilde{l} = \tilde{y}_2 - \tilde{y}_1$, the dimensionless velocities of both steps are given by

$$\frac{\mathrm{d}\tilde{y}_1}{\mathrm{d}\tilde{t}} = \frac{(\cosh\tilde{l} + \lambda_- \sinh\tilde{l}\,)(\tilde{f} - \tilde{l}^{-3}) - (\tilde{f} + \tilde{l}^{-3})}{(\lambda_- + \lambda_+)\cosh\tilde{l} + (1 + \lambda_-\lambda_+)\sinh\tilde{l}} + \frac{1}{1+\lambda_-}(\tilde{f} - \tilde{l}^{-3}) \tag{5.1}$$

$$\frac{d\tilde{y}_2}{d\tilde{t}} = \frac{(\cosh\tilde{l} + \lambda_+ \sinh\tilde{l}\,)(\tilde{f} + \tilde{l}^{-3}) - (\tilde{f} - \tilde{l}^{-3})}{(\lambda_- + \lambda_+)\cosh\tilde{l} + (1 + \lambda_-\lambda_+)\sinh\tilde{l}} + \frac{1}{1+\lambda_+}(\tilde{f} + \tilde{l}^{-3}). \quad (5.2)$$

By combining eqs. (5.1) and (5.2), the change of the step distance is given by

$$\frac{d\tilde{l}}{d\tilde{t}} = \frac{(\lambda_-^2 - \lambda_+^2)\tilde{f}e^{-\tilde{l}} + F(\tilde{l})\tilde{l}^{-3}}{[(\lambda_- + \lambda_+)\cosh\tilde{l} + (1 + \lambda_-\lambda_+)\sinh\tilde{l}](1+\lambda_+)(1+\lambda_-)}, \quad (5.3)$$

where

$$F(\tilde{l}) = [(2 + \lambda_+ + \lambda_-)(1 + \lambda_+\lambda_-) + (1+\lambda_+)(1+\lambda_-)(\lambda_+ + \lambda_-)]\sinh\tilde{l} + [(2 + \lambda_+ + \lambda_-)(\lambda_+ + \lambda_-) + 2(1+\lambda_+)(1+\lambda_-)]\cosh\tilde{l} + 2(1+\lambda_+)(1+\lambda_-). \quad (5.4)$$

In the steady state, $d\tilde{l}/d\tilde{t} = 0$, $\tilde{f}$ satisfies

$$\tilde{f} = -\frac{e^{\tilde{l}}F(\tilde{l})\tilde{l}^{-3}}{\lambda_-^2 - \lambda_+^2}. \quad (5.5)$$

If $\lambda_- \gg \lambda_+$, the stability boundary in $\tilde{f}$-$\tilde{l}$ diagram is similar to Fig. 1 of ref. 20. When the undersaturation exceeds a critical value, there appear two steady step distances $\tilde{l}_s$ and $\tilde{l}_u$ ($\tilde{l}_s < \tilde{l}_u$): $\tilde{l}_s$ is the stable and $\tilde{l}_u$ is unstable. When the initial step distance is larger than $\tilde{l}_u$, the repulsion between steps overcomes the attractive force by the surface diffusion field, and the steps separate. When the initial step distance is smaller than $\tilde{l}_u$, the step distance becomes $\tilde{l}_s$ and a stable pair is formed. At the critical undersaturation, $\tilde{l}_s$ and $\tilde{l}_u$ coincide and the critical step distance $\tilde{l}_c$ is determined by $d\tilde{f}/d\tilde{l} = 0$ with eq. (5.4). The critical pair size $\tilde{l}_c$ is insensitive to the kinetic coefficients, and mainly determined by the form of step interaction, for example $\tilde{l}_c \approx 3/2$ with the elastic repulsion ($\nu = 2$). The critical undersaturation strongly depends on the asymmetry of the step kinetics, and expressed as

$$\tilde{f}_c \approx \begin{cases} -\frac{8e^3}{27}\frac{\lambda_- + \lambda_+}{(\lambda_- - \lambda_+)} & (\lambda_+ + \lambda_- \gg \lambda_+\lambda_- \gg 1) \\ -\frac{8e^3}{27}\frac{\lambda_+\lambda_-}{(\lambda_- - \lambda_+)} & (\lambda_+\lambda_- \gg \lambda_+ + \lambda_- \gg 1) \\ -\frac{16(e^3 + e^{3/2})}{27(\lambda_-^2 - \lambda_+^2)} & (1 \gg \lambda_+ + \lambda_- \gg \lambda_+\lambda_-). \end{cases} \quad (5.6)$$

The critical undersaturation becomes very large if asymmetry is weak. Thus a strong asymmetry is necessary for the pairing.

5.2 *Formation of three-body bound state*

Although simple bound state of more than three steps does not appear in the one-sided model, it is observed in real systems.[1)] Since conditions for the formation of a three-body bound state are in general not simple, we have to rely on numerical calculation. Figure 4 shows the parameter region of $\lambda_\pm$ for the formation of three-body bound state. When the undersaturation is sufficiently large, a three-body bound state appears if $\lambda_\pm$ is small and very asymmetric. As the undersaturation increases, the parameter area for the three-body bound state becomes larger. The maximum values of λ_+ and λ_- in this region are approximately proportional to $\tilde{f}^{1/3}$. This simple relation is valid when the undersaturation is large so that the step distances in the bound state are much smaller than the surface diffusion length.

In some limiting cases we can study conditions for the formation of three-body bound state analytically. From numerical analysis we learned that the three-body bound state is formed in the same way with repulsion only between nearest neighbor steps. Therefore nearest neighbor interaction is essential. For simplicity we assume that the step repulsion acts only between nearest neighbors, and strong asymmetry in kinetics as $\lambda_+ = 0$ and $\lambda_- \gg 1$. When there are only three steps, Step 1, Step 2 and Step 3 at $\tilde{y}_1$, $\tilde{y}_2$ and $\tilde{y}_3$ ($\tilde{y}_1 < \tilde{y}_2 < \tilde{y}_3$) on the surface with small distances $\tilde{l}_1 (= \tilde{y}_2 - \tilde{y}_1)$ and $\tilde{l}_2 (= \tilde{y}_3 - \tilde{y}_2)$ such that $\lambda_-\tilde{l}_1$, $\lambda_-\tilde{l}_2 \ll 1$, the velocities of the steps are approximately given by

$$\frac{d\tilde{y}_1}{d\tilde{t}} = \frac{2}{\lambda_-}\left(\tilde{f} - \frac{1}{\tilde{l}_1^3}\right) - \frac{1}{\lambda_-}\left(\tilde{f} + \frac{1}{\tilde{l}_1^3} - \frac{1}{\tilde{l}_2^3}\right), \quad (5.7)$$

$$\frac{d\tilde{y}_2}{d\tilde{t}} = \frac{3}{\lambda_-}\left(\frac{1}{\tilde{l}_1^3} - \frac{1}{\tilde{l}_2^3}\right), \quad (5.8)$$

$$\frac{d\tilde{y}_3}{d\tilde{t}} = \left(\tilde{f} + \frac{1}{\tilde{l}_2^3}\right) - \frac{1}{\lambda_-}\left(\tilde{f} + \frac{1}{\tilde{l}_1^3} - \frac{1}{\tilde{l}_2^3}\right). \quad (5.9)$$

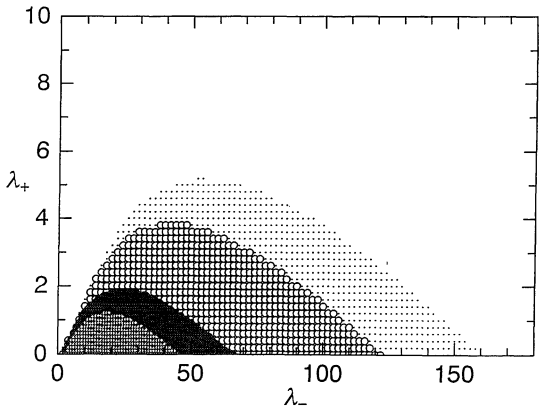

Fig. 4. Parameter region where the three-body bound state appears. The different hatching represents various undersaturation. $\tilde{f} = -0.8^3 \times 10^4$, -1.0×10^4, $-1.6^3 \times 10^4$, $-2.0^3 \times 10^4$, for the increasing order.

Once a bound state is formed, the three steps move steadily: $d\tilde{l}_1/d\tilde{t} = 0$ and $d\tilde{l}_2/d\tilde{t} = 0$. These two conditions determine the step distances as

$$\tilde{l}_1^* = 2^{1/3}|\tilde{f}|^{-1/3}, \tag{5.10}$$

$$\tilde{l}_2^* = |\tilde{f}|^{-1/3}. \tag{5.11}$$

The stability of this configuration is tested by giving a small perturbation $\delta\tilde{l}_1$ to the upper terrace and observing if the first step escapes. From eqs. (5.7), (5.8) and (5.9), the dimensionless growth rate of the perturbation $\tilde{\omega}$ is given by

$$\tilde{\omega} = \frac{3}{\lambda_-}\left(\lambda_- - \frac{6}{\tilde{l}_1}\right)\frac{1}{\tilde{l}_1^3}. \tag{5.12}$$

Thus for the three-body bound state to be stable, λ_- needs to be smaller than the critical value,

$$\lambda_-^* = 6\left(\frac{|\tilde{f}|}{2}\right)^{1/3}. \tag{5.13}$$

The above relation and the ratio of the distances obtained from eqs. (5.10) and (5.11), $\tilde{l}_1^*/\tilde{l}_2^* = 2^{1/3}$ agree with the numerical result for large undersaturation.

In the above configuration, the local undersaturations at the three steps satisfy the relation, $\tilde{f}_2 > \tilde{f}_1 > \tilde{f}_3$. In the one-sided model the distribution of the adatom density is shown in Fig. 5(a). With an increase of the upper step distance $\tilde{l}_1$ (the left side is higher than the right), Step 1 increases the area on the right, where Step 1 emits atoms, but Step 2 does not increase its area on the right. Consequently Step 1 increases the velocity, and Step 2 cannot catch up with Step 1. Therefore the three-body bound state is unstable in the one-sided model. On the other hand when the three-body bound state is formed with $\lambda_- < \lambda_-^*$, the distribution of the adatom density is very different as shown in Fig. 5(b). Step 2 emits atoms onto terraces on both sides, and Step 1 absorbs atoms from the terrace on the right. With an increase of the step distance $\tilde{l}_1$, Step 2 increases the area for emitting atoms while Step 1 increases the area for absorbing adatoms. Consequently Step 1 decreases the velocity and Step 2 increases the velocity. Therefore Step 2 can catch up with Step 1 and the three-body bound state is stable.

Near the critical resistance λ_-^*, strange behavior is observed. When λ_- is slightly larger than λ_-^* two step pairs oscillate as shown in Fig. 6. The lower side pair on the right is faster than the upper side pair, and they collide. At first the upper step in the upper pair is expelled. Since the three-body bound state is unstable with this parameters, the three steps left behind cannot form a three-body bound state, and the next step is expelled too. Since the lower step is faster than the upper step, they form a step pair again. And the whole process is repeated; the collision of two pairs, the collapse of the upper pair and the reformation of the upper pair.

In the numerical simulation a four-body bound state is formed with an increase of undersaturation. The parameter region is similar to that for a three-body bound state. Though we have no evidence, bound state consisting of more steps may be possible with extremely large unrealistic undersaturation when the step kinetics are fast and the Schwoebel effect is sufficiently large.

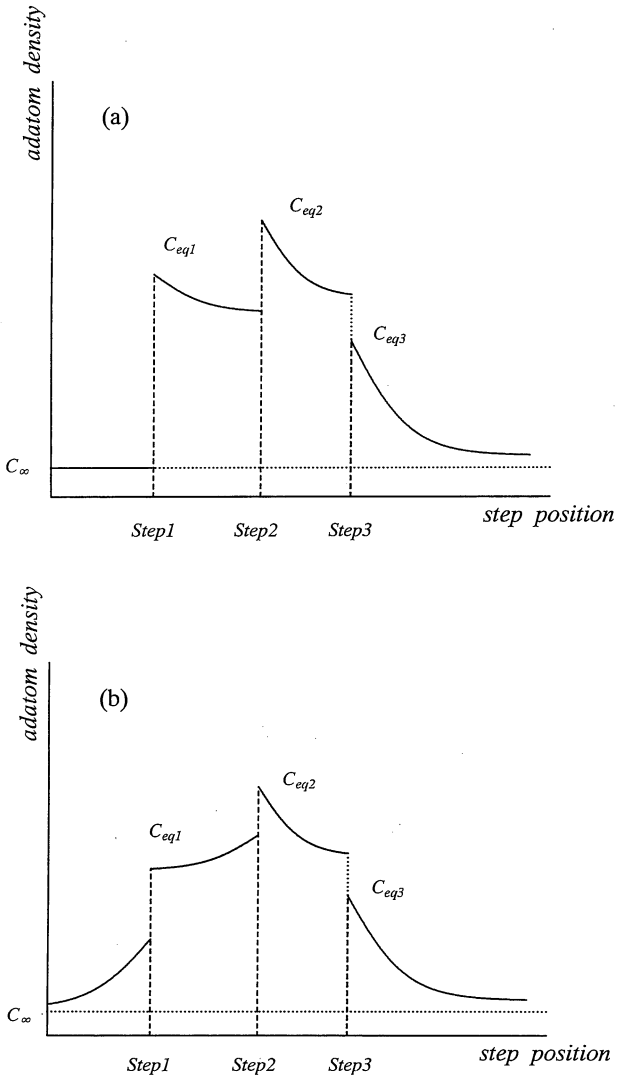

Fig. 5. (a)Schematic distribution of adatom density in the one-sided model. (b)Schematic distribution of adatom density when the three-body bound state is formed.

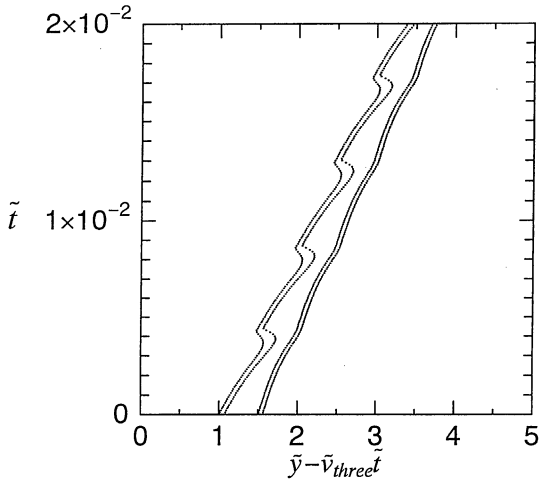

Fig. 6. The oscillation of the two step pairs in the moving frame with a velocity of three-body bound state when $\lambda_+ = 2$, $\lambda_- = 40$ and $\tilde{f} = -10^4$.

5.3 Velocity of a step pair and a three body bound state

The velocity of an isolated step is proportional to the undersaturation and given by eq. (2.6) as

$$\tilde{v} = \frac{(2+\lambda_+ + \lambda_-)\tilde{f}}{(1+\lambda_+)(1+\lambda_-)}. \tag{5.14}$$

When a step pair is formed, the step distance and the undersaturation satisfy eq. (5.5). In the large undersaturation the step distance is very small, and given by

$$\tilde{l} \approx \left[\frac{(2+\lambda_+ +\lambda_-)(\lambda_+ +\lambda_-)+4(1+\lambda_+)(1+\lambda_-)}{(\lambda_+ - \lambda_-)(\lambda_+ + \lambda_-)\tilde{f}}\right]^{1/3}. \tag{5.15}$$

The resultant velocity of the pair is

$$\tilde{v}_{\text{pair}} \approx \frac{4(1+\lambda_+ + \lambda_-)\tilde{f}}{(2+\lambda_+ + \lambda_-)(\lambda_+ + \lambda_-) + 4(1+\lambda_+)(1+\lambda_-)}. \tag{5.16}$$

This result is different from that of the one-sided model,[20] where the velocity of a step pair is proportional to $|\tilde{f}|^{2/3}$. In the one-sided model the velocity of the upper step is determined by the diffusion current on the lower side terrace. The terrace width between the steps is determined by the competition between the surface diffusion and the repulsion, and the velocity depends on the form of the repulsion. In the present case the velocity of the upper step is determined by the surface diffusion for both side terraces. With the large $|\tilde{f}|$ the surface diffusion onto the left upper terrace finally dominates and recovers the linear dependence of the velocity on $\tilde{f}$. By using eqs. (5.10) and (5.11), the velocity of the three-body bound state in $\lambda_+ = 0$ and $\lambda_- \gg 1$ is also obtained as

$$\tilde{v}_{\text{three}} \approx \frac{3}{2\lambda_-}|\tilde{f}|. \tag{5.17}$$

Figure 7 shows the dependence of these velocities on the undersaturation obtained by numerical simulation. A solid line, a broken line and a dotted chain line represent the velocity of an isolated step, a step pair and a three-body bound state. The velocity of an isolated step is always proportional to the undersaturation, which agrees with eq. (5.14). The step pair appears when $|\tilde{f}|$ is about 10. Near the critical undersaturation the velocity of the step is not proportional to $|\tilde{f}|$ but to $|\tilde{f}|^{3/2}$. With an increase of the undersaturation, the velocity of the step pair gradually becomes proportional to $|\tilde{f}|$. From the above argument we expect that the velocity of an n-body bound state is also proportional to the undersaturation if the $|\tilde{f}|$ is sufficiently large.

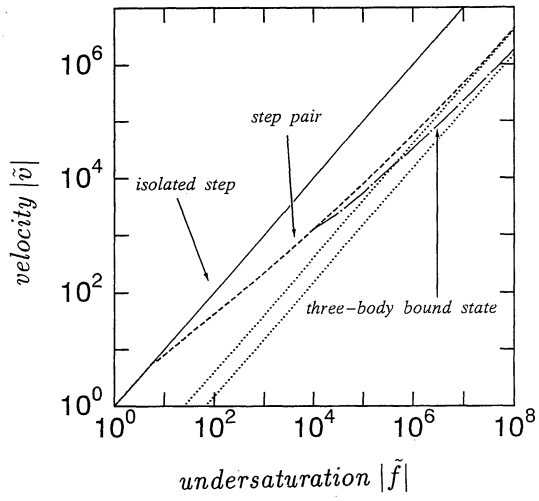

Fig. 7. Dependence of the velocities of bound states on undersaturation. With an increase of undersaturation, each line approaches gradually to the one of dotted lines, which are proportional to $|\tilde{f}|$.

§6. Summary

In this paper we studied the change of the character of bound states by the change of the strength of asymmetry in the step kinetics. As regard to the formation of a step pair, the strength of asymmetry affects mainly on the critical undersaturation. The critical undersaturation becomes larger as the asymmetry decreases. Except that, the condition for the pair formation in the general asymmetric model is similar to the one-sided model. The drastic changes appear in the many step system. With a certain asymmetry, many-body bound states, which do not appear in the one-sided model, can exist stably. They appear when the step kinetics is fast and the asymmetry of step kinetics for both side terraces is sufficiently large. The parameter region of $\lambda_\pm$ where the many-body bound state is stable becomes large with increasing of undersaturation. The upper limit of λ_- is proportional to $|\tilde{f}|^{1/3}$, of which the exponent depends on the form of step repulsion.

In the general asymmetric case near the critical point, the most unstable mode for an equidistant step train is in the long wavelength, which is in contrast to the pairing instability in the one-sided model. As a result of competition between the repulsion and the surface diffusion, the fastest growing fluctuation of a particular wavelength is selected. The density modulation of steps induced by the instability moves slowly in the same direction as the steps, and its amplitude grows exponentially as the Mullins-Sekerka instability.[33] When the amplitude of fluctuation becomes large, nonlinear effects come into play. Taking account of the nonlinear effect near the critical undersaturation, the evolution equation of step density obeys the Benney equation with a large dispersion term. This result corresponds to the appearance of an array of equidistant bunches. The predicted profile exhibits a sharp change of step density at the lower side and a gradual change at the upper side.

In this paper we have assumed $\lambda_- > \lambda_+$. If the Schowebel effect is opposite, $\lambda_+ > \lambda_-$, that is, the adatoms on the upper terrace are incorporated into the step more easily than that on the lower terrace, bunching occurs in growth above a critical supersaturation since the problem is symmetric with the change of variables $y \to -y$, and $\tilde{f} \to -\tilde{f}$.

Although we do not yet have a clear example of bunching in sublimation by the Schwoebel effect, step bunching observed in growing crystals such as GaAs[40] and SiC[41] are also the candidates of the present mechanism.

Acknowledgments

M. U. thanks Y. Saito for useful discussions. The present work is partially supported by the Grant-in-Aid from Japanese Ministry of Education. The authors are benefited by the interuniversity cooperative research program of IMR, Tohoku University.

1) A. V. Latyshev, A. L. Aseev, A. B. Krasilnikov and S. I. Stenin: Surf. Sci. **213** (1989) 157.
2) A. V. Latyshev, A. L. Aseev, A. B. Krasilnikov and S. I. Stenin: Surf. Sci. **227** (1990) 24.
3) Y. Homma, R. J. Mcclelland and H. Hibino: Jpn. J. Appl. Phys. **29** (1990) L2254.
4) S. Stoyanov: Jpn. J. Appl. Phys. **30** (1991) 1.
5) A. Natori: Jpn. J. Appl. Phys. **33** (1994) 3538.
6) B. Houchmandzadeh, C. Misbah and A. Pimpinelli: J. Phys. I France **4** (1994) 1843.
7) D. Kandel and E. Kaxiras: Phys. Rev. Lett. **76** (1996) 1114.
8) C. Misbah, O. Pierre-Louis and A. Pimpinelli: Phys. Rev. B **51** (1995) 17283.
9) C. Misbah and O. Pierre-Louis: Phys. Rev. E **53** (1996) R4318.
10) M. Sato and M. Uwaha: J. Phys. Soc. Jpn. **65** (1996) 1515.
11) D. J. Benney: J. Math. Phys. **45** (1966) 150.
12) T. Kawahara: Phys. Rev. Lett. **51** (1983) 381.
13) T. Kawahara and M. Takaoka: Physica D **39** (1989) 43.
14) T. Kawahara and S. Toh: Phys. Fluids **31** (1988) 2103.
15) Y. Kuramoto and T. Tsuzuki: Prog. Theor. Phys. **55** (1976) 356.
16) G. I. Sivashinsky: Acta Astronaut. **4** (1977) 1177.
17) P. Manneville: *Propagation in Systems Far From Equilibrium*, ed. J. E. Wesfreid *et al.* (Springer, Berlin, 1988) p. 265.
18) R. L. Schwoebel and E. J. Shipsey: J. Appl. Phys. **37** (1966) 3682.
19) R. L. Schwoebel: J. Appl. Phys. **40** (1969) 614.
20) M. Uwaha: Phys. Rev. B **46** (1992) 4364.
21) M. Uwaha: J. Cryst. Growth **128** (1993) 92.
22) M. Sato and M. Uwaha: Phys. Rev. B **51** (1995) 11172.
23) M. Sato and M. Uwaha: Europhys. Lett. **38** (1995) 639.
24) W. K. Burton, N. Cabrera, and F. C. Frank: Philos. Trans. R. Soc. London Ser A **234** (1951) 299.
25) Y. Saito and M. Uwaha: Phys. Rev. B **49** (1994) 10677.
26) A. Pimpinelli, I. Elikinani, A. Karma, C. Misbah and J. Villain: J. Phys.: Condens. Matter **6** (1994) 2661.
27) D. Kandel and J. D. Weeks: Phys. Rev. Lett. **74** (1995) 3632.
28) B. S. Bales and A. Zangwill: Phys. Rev. B **41** (1990) 5500.
29) W. W. Mullins: *Metal Surfaces*, ed. W. D. Robertson and N. A. Gjostein (Metall. Soc. AIME, Metals Park, 1963).
30) V. I. Marchenko and A. Ya. Parshin: Zh. Eksp. Teor. Fiz. **79** (1980) 257; translation: Sov. Phys. JETP **52** (1980) 129.
31) F. Liu and H. Metiu: Phys. Rev. E **49** (1994) 2601.
32) G. Ehrich and F. G. Hudda: J. Chem. Phys. **44** (1966) 1039.
33) W. W. Mullins and R. F. Sekerka: J. Appl. Phys. **34** (1963) 323.
34) M. Uwaha and P. Nozières: *Morphology and Growth Unit of Crystals*, ed. I. Sunagawa (Terra Scientific, Tokyo, 1989) p. 17.
35) P. Nozières: *Solid Far from Equilibrium*, ed. C. Godrèche (Cambridge Univ. Press, Cambridge, 1992) p. 1.
36) I. Bena, C. Misbah and A. Valance: Phys. Rev. B **47** (1993) 7408.
37) In ref. 10 we wrote that the bunch recedes with a sharp front and a smooth end in negative δ, which is wrong.
38) M. Uwaha, Y. Saito and M. Sato: J. Cryst. Growth **146** (1995) 164.
39) W. W. Mullins and J. P. Hirth: J. Chem. Phys. Solids **44** (1963) 1391.
40) H. W. Ren, X. Q. Shen and T. Nishinaga: J. Cryst. Growth **166** (1996) 217.
41) T. Kimoto, A. Itoh and H. Matsunami: Appl. Phys. Lett. **66** (1995) 3645.